Brain Pathology ISSN 1015-6305

RESEARCH ARTICLE

LGR5 is a Marker of Poor Prognosis in Glioblastoma and is Required for Survival of Brain Cancer Stem-Like Cells

Susumu Nakata[1]*; Benito Campos[2]; Josephine Bageritz[1]; Justo Lorenzo Bermejo[3,4]; Natalia Becker[1]; Felix Engel[1]; Till Acker[5]; Stefan Momma[6]; Christel Herold-Mende[2]; Peter Lichter[1]; Bernhard Radlwimmer[1]; Violaine Goidts[1]

[1] Division of Molecular Genetics, German Cancer Research Center, Heidelberg.
[2] Division of Neurosurgical Research, Department of Neurosurgery, University of Heidelberg, Heidelberg.
[3] Institute of Medical Biometry and Informatics, University Hospital Heidelberg, Heidelberg.
[4] Division of Molecular Genetic Epidemiology, German Cancer Research Center, Heidelberg.
[5] Institute of Neuropathology, University Hospital Giessen und Marburg GmbH, Giessen.
[6] Neurological Institute (Edinger Institute), Frankfurt University Medical School, Frankfurt am Main.

Keywords
apoptosis, cancer stem cell, glioblastoma, glioma, *LGR5*.

Corresponding author:
Violaine Goidts, PhD, Division of Molecular Genetics, German Cancer Research Center, Im Neuenheimer Feld, 280, 69120, Heidelberg, Germany (E-mail: *v.goidts@dkfz.de*)

Received 5 April 2012
Accepted 6 July 2012
Published Online Article Accepted 16 July 2012

* Current adress: Division of Oncological Pathology, Aichi Cancer Center Research Institute, Nagoya, Japan

doi:10.1111/j.1750-3639.2012.00618.x

Abstract

In various types of cancers including glioblastoma, accumulating evidence show the existence of cancer stem-like cells (CSCs), characterized by stem cell marker expression, capability of differentiation and self-renewal, and high potential for tumor propagation *in vivo*. *LGR5,* whose expression is positively regulated by the Wnt signaling pathway, is a stem cell marker in intestinal mucosa and hair follicle in the skin. As Wnt signaling is also involved in brain development, the function of *LGR5* in the maintenance of brain CSCs is to be assessed. Our study showed that the *LGR5* transcript level was increased in CSCs. Co-immunofluorescence staining demonstrated the co-localization of CD133- and LGR5-positive cells in glioblastoma tissue sections. Functionally, silencing of *LGR5* by lentiviral shRNA-mediated knockdown induced apoptosis in brain CSCs. Moreover, LGR5 depletion led to a downregulation of L1 cell adhesion molecule expression. In line with an important function in glioma tumorigenesis, LGR5 expression increased with glioma progression and correlated with an adverse outcome. Our findings suggest that LGR5 plays a role in maintenance and/or survival of brain CSCs.

INTRODUCTION

In glioma, accumulating evidence support the existence of a small subpopulation of cancer cells with properties of neural stem cells (NSC), including the expression of stem cell markers, as well as the capability to differentiate and self-renew (16, 24, 34, 35). In addition, these cancer stem-like cells (CSCs) have a high tumorigenic potential and are resistant to chemotherapy and irradiation, suggesting that cancer cells harboring stem cell-like properties might be responsible for tumor development, recurrence and metastasis (2, 32, 38). A recent study using a transgenic mouse glioma model provided evidence that neural stem/progenitor cells with accumulation of genetic aberrations can be the origin of malignant astrocytoma (1). Further investigation of the molecular mechanisms that regulate CSCs expansion and maintenance is, therefore, essential to better understand glioma pathology and develop novel and effective therapeutics. However, the lack of specific stem cell markers impedes the isolation and analysis of glioblastoma stem-like cells.

In the recent years, several reports highlighted restricted expression of the leucine-rich repeat containing G-protein–coupled receptor 5 (LGR5) in a small subset of cells from the intestinal crypt bottom, also found in stomach and hair follicles (4, 5, 26). *LGR5* expression is positively regulated by the Wnt signaling pathway (4, 36), which is an essential pathway in brain development, regulating expansion and maintenance of neural stem and precursor cell populations (15, 29). Notably, Wnt signaling is also involved in the tumorigenesis of various other cancers (11, 25). Recently, it has been reported that the secreted Wnt-enhancer proteins R-spondins interact with LGR4 and LGR5, regulating Wnt signaling (9, 12, 20).

Despite the eminent role of Wnt signaling in tumorigenesis, the functional role of LGR5 in brain tumors has not yet been examined. In this study, we investigated the expression pattern of LGR5 in clinical samples of astrocytoma tumors of different World Health Organization (WHO) grades and studied its function in survival and maintenance of brain CSCs *in vitro*.

MATERIALS AND METHODS

Cell culture

Glioblastoma samples were obtained from patients undergoing surgical resection according to the research proposals approved by the Institutional Review Board at the Medical Faculty of Heidelberg, Germany. Tissues were enzymatically dissociated and cultivated in stem cell medium as neurospheres (13, 14), made of Dulbecco's modified Eagle's medium (DMEM)/F-12 medium containing 20% bovine serum albumin, insulin, transferrin (BIT) serum-free supplement, basic fibroblast growth factor and epidermal growth factor (EGF) at a concentration of 20 ng/mL each (Invitrogen, Karlsruhe, Germany). The brain CSC lines NCH421k and NCH441 cells were established independently from patients-derived tumors of glioblastoma multiforme, and characterized genotypically and phenotypically in previous studies (8, 10, 14). To induce differentiation, neurospheres were grown in DMEM medium containing 10% fetal calf serum and 10 nM all-trans retinoic acid (ATRA) after dissociation of neurospheres by trypsin (NCH421k) or accutase (NCH441). Human normal astrocytes were purchased from Promocell (Heidelberg, Germany) and maintained in astrocyte basal medium with astrocyte growth supplement, 2% fetal bovine serum and 1/3 conditioning medium (ScienCell, Carlsbad, CA, USA), according to supplier's recommendation.

Lentiviral vector-mediated short hairpin RNA interference

RNAi clones targeting *LGR5* were purchased from Sigma-Aldrich (St Louis, MO, USA) (TRCN0000011585, TRCN0000011586, TRCN0000011587). Lentiviral particles were produced according to the manufacturer's instruction. Lentiviruses were concentrated by ultracentrifugation. Titer was measured by detecting green fluorescent protein (GFP)-positive HEK293T cells using flow cytometry. Before transduction, neurospheres were dissociated with trypsin or accutase treatment. Transductions were performed at five of multiplicity of infection with 8 μg/mL polybrene for brain CSCs, conferring ~90 % transduction efficiency without significant cytotoxicity in negative control samples.

Quantitative real-time polymerase chain reaction (qRT-PCR)

One μg of total RNA was treated with DNaseI (Invitrogen) and reverse-transcribed with SuperscriptII (Invitrogen). Each complementary DNA sample was analyzed in triplicate with the ABI PRISM 7700 (Applied Biosystems, Foster City, CA, USA) using Absolute SYBR Green ROX Mix (ABgene, Epsom, UK) according to the manufacturer's instructions. Two endogenous housekeeping genes (*ARF1* and *DCTN2*) were used as internal standards. All primers were tested to exclude amplification from genomic DNA. Pooled total normal brain extract from five adult donors were purchased (BioChain Institute, Inc., Hayward, CA, USA) and used as control. The relative quantification of the RNA of interest in comparison with the housekeeping genes was calculated with the standard curves that were generated with serial 1:3 dilutions of cDNA sample from the universal human reference total RNA (Stratagene Agilent Technologies, West Cedar Creek, TX, USA). Oligonucleotide sequences are available in Supporting Information Table S1.

Immunohistochemistry and immunofluorescence staining

Spheroid cells were dissociated by trypsin. Differentiation-induced cells were detached from plates by trypsin and washed in PBS. Cytospin smears were prepared using Cytospin 3 Cytocentrifuge (Wolf Laboratories Limited, Pocklington, UK) and fixed with 4 % paraformaldehyde for 10 min at room temperature followed by permeablization using 0.01% of Triton X. Paraffin-embedded sections were deparaffinized in xylene, and rehydrated through descending concentrations of ethanol. Antigen retrieval was performed using citrate buffer (10 mM, pH 6.0) and heating in a steamer cooker for 40 minutes. Endogenous peroxidase was blocked by 3% hydrogen peroxide for 10 minutes. Twenty percent normal goat serum was used as blocking solution for the LGR5 staining. Nuclei were counterstained with hematoxylin for 1 minute. LGR5 polyclonal antibodies (MBL International, Woburn, MA, USA, LS-A1235 at 1:50, or LS-A1232 at 1:100), and monoclonal CD133/1 antibody (Miltenyi Biotec, Bergisch Gladbach, Germany, at 1:11 dilution) were incubated overnight at 4°C. Immunohistochemical analysis including tissue microarray was performed using Envision+ System and AEC or DAB visualization (Dako, Carpinteria, CA, USA) according to the manufacturer's instructions.

Co-immunofluorescence staining was performed using CSAII Signal Amplification System (Dako) for CD133 and Alexa Fluor 568-conjugated goat anti-rabbit IgG (Invitrogen, Carlsbad, CA, USA) as secondary antibody for LGR5. Nuclei were stained using To-Pro3 prior to mounting. Negative controls were obtained with the same procedure without primary antibody or unimmunized rabbit IgG (Dako).

Cell viability and apoptosis assays

Cell viability was quantified with CellTiter Glo Luminescent Cell Viability Assay kit according to manufacturer's instruction (Promega, Madison, WI, USA). Cell counting with trypan blue dye exclusion test was performed with standard protocol using Vi-CELL counter (Beckman Coulter, Fullerton, CA, USA). Apoptosis was quantified using the subG1 hypodiploid apoptosis assay. Cells were fixed with 70% ethanol, treated with ribonuclease A (SIGMA Chemical Co., St Louis, MO, USA), and the nuclei were stained with propidium iodide (SIGMA Chemical Co.). The DNA content was measured using a FACSCanto flow cytometer with FACSDiva software (BD Biosciences, San Jose, CA, USA). For all assays, 10 000 cells were counted.

Tissue microarray

Tumor samples for the tissue microarray were collected at the Department of Neurosurgery, Heidelberg University Hospital, Germany. Eligibility criteria included written informed consent from the patient and availability of follow-up data. All patients were treated by surgery at diagnosis; radiotherapy and/or chemotherapy were administered for high-grade tumors. All tumors were

classified according to the WHO Classification of Tumors of the Nervous System. The LGR5 staining score was assessed by two independent researchers, who were blind to clinical informations. Average staining of evaluable biopsies of each individual patient were taken as final result. Complete negative staining was defined as LGR5 score 1. Cases containing only rare positive cells (~10%) were defined as score 2. Cases containing 10~70% LGR5-positive cells were defined as score 3. Cases in which the vast majority of cells (>70%) were LGR5 positive were defined as score 4. We defined LGR5 "low" as cases with scores 1 and 2, and LGR5 "high" as cases with scores 3 and 4.

Patient characteristics of all samples used for the TMA are summarized in Supporting Information Table S2.

Gene expression analysis

Sample amplification was done using 100 ng of total RNA by the method of Van Gelder *et al* (37). RNA was amplified using the TotalPrep RNA Amplification kit (Illumina, San Diego, CA, USA) following the manufacturer's instructions. Labeling was achieved by incorporation of biotin-16-uridine triphosphate (UTP). Labeled RNA was hybridized to the Illumina Human whole genome Sentrix-6 V2 BeadChip array according to the manufacturer's instructions (Illumina). Microarray scanning was done using a Beadstation array scanner. Data extraction was done using the bead array R package (svn release 1.7.0) from bioconductor.org. Bead outliers were removed when their expression value dropped below a threshold, because of the imaging system background, nonspecific binding or cross-hybridization signal. Individual bead types were flagged as filtered when their bead replicate count dropped below 17. We excluded a bead type when its filter flag was set across all samples. Data analysis was done by variance stabilizing and spline normalizing the signals using the algorithms from the lumi R package (release 1.1.0) from bioconductor.org (19), implemented in our in-house developed ChipYard framework for microarray data analysis (http://www.dkfz.de/genetics/ChipYard).

R2, a microarray analysis and visualization platform, provided by the Department of Human Genetics of the Academic Medical Centre (Amsterdam, the Netherlands; http://r2.amc.nl), was used to study *LGR5* mRNA expression in CD133 sorted glioblastoma cells [(17) GSE18015; n = 8]. Expression data was MAS5.0 normalized prior to analysis.

Statistical analysis

Significance analysis of microarrays (SAM) was performed using the MeV software (31), applying a false discovery rate < 1%. Genes showing a q-value < 1% were considered as significantly differentially expressed between negative controls and shRNA-*LGR5*–transduced samples.

Correlation between LGR5 expression and tumor aggressiveness was expressed as Pearson's correlation coefficients. The association between overall survival and gene expression was calculated using log-rank tests and presented as Kaplan–Meier plots. Multivariate survival statistics were performed employing multivariate Cox regression. Calculations were performed using the statistical software environment R, version 2.4.1 (http://www.r-project.org).

RESULTS

LGR5 is expressed in brain CSCs

Several reports have emphasized the role of *LGR5* as a stem cell marker in various tissues (4, 5, 22, 26). In order to verify its possible use to characterize brain CSCs, we examined *LGR5* mRNA expression levels in CSCs of glioblastoma. As shown in Figure 1A, CSCs expressed *LGR5* mRNA up to 10-fold higher when compared with cultured normal astrocytes and total normal brain extract, suggesting a stem-like cell-specific high-level expression. Moreover, *LGR5* mRNA expression in glioblastoma cells sorted for their CD133 content was determined by *in silico* analysis of publicly available microarray data (17), using R2 analysis software. *LGR5* expression was found to correlate with CD133 content ($r = 0.582$, $P = 0.02$, Figure 1B). In order to study LGR5 protein expression in glioblastoma tissues, we first confirmed the specificity of anti-LGR5 antibody using human normal small intestine tissue sections, demonstrating its exclusive expression in the crypt base columnar cells consistent with a previous report (4) (Figure 1C). Immunohistochemical staining of glioblastoma sections showed LGR5-positive tumor cells to be preferentially localized in the vicinity of blood vessels, reminiscent of the perivascular niche of CSCs previously described for CD133 positive cells (7, 33) (Figure 1D). Given the putative role of LGR5 as stem cell marker, we investigated the overlap of LGR5 and CD133 protein expression by co-immunofluorescence staining with anti-CD133 and anti-LGR5 antibody. As depicted in Figure 1E, CD133 protein expression co-localized with LGR5 in glioblastoma tissue samples, suggesting that these markers could identify a small subpopulation of brain CSCs.

LGR5 is downregulated upon differentiation

To verify the stem cell specificity of LGR5 expression, we induced differentiation of CSCs (Figure 2A) by cultivating glioblastoma spheroids in ATRA-containing medium without growth factors. Differentiation was indicated by the observed decreased *CD133* expression and increased *GFAP* expression (Figure 2B). Importantly, *LGR5* mRNA expression was reduced by more than twofold in ATRA-treated cells when compared with undifferentiated cells (Figure 2B). Moreover, LGR5-positive cells were similarly reduced following ATRA treatment. In contrast, the proportion of GFAP-positive cells was increased indicating differentiation of ATRA-treated cells. These results confirmed that LGR5 is expressed preferentially in brain CSCs and is reduced following differentiation (Figure 2C).

LGR5 knockdown suppresses viability and induces apoptosis of brain CSCs

Given the association of *LGR5* expression with stem cell characteristics, we hypothesized that *LGR5* might play a role in brain CSCs maintenance. To test this, we silenced *LGR5* mRNA expression using lentiviral-mediated shRNA and confirmed the successful knockdown by qRT-PCR (Figure 3A) and immunofluorescence staining (Figure 3B). Upon *LGR5* silencing, the spheroid morphology of brain CSCs was impaired (Figure 3C). The growth curve by trypan blue dye exclusion test demonstrated that *LGR5*

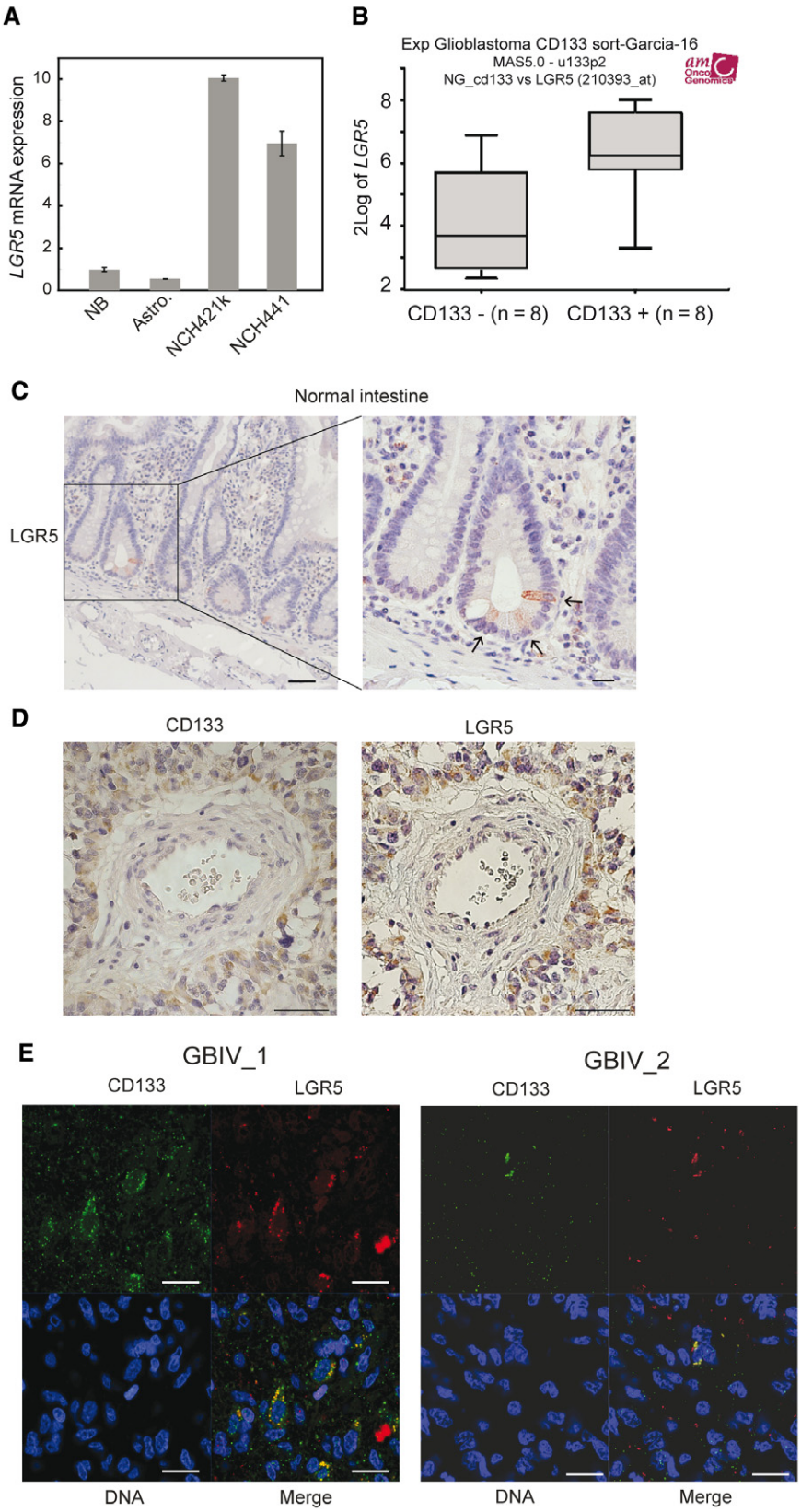

Figure 1. *LGR5 is expressed in brain CSCs* in vitro *and in CD133*$^{+}$ *cells in glioblastoma.* **A.** Analysis of *LGR5* mRNA expression by quantitative real-time polymerase chain reaction. Total mRNA was extracted from NB, Astro and brain CSCs (NCH421k and NCH441). Results were normalized to *mRNA* levels of two housekeeping genes. Error bars represent standard deviations of three independent biological replicates. **B.** *In silico* analysis of *LGR5* mRNA expression using R2 analysis software on datasets of CD133 sorted glioblastoma cells. **C.** Normal intestine labelling was used as positive control for LGR5 antibody. Isotype. Scale bar = 50 μm for left panel, 20μm for center and right panel. **D.** Representative images of LGR5 and CD133 positive perivascular glioblastoma cells. Scale bar = 50 μm. **E.** Representative images of co-immunofluorescence staining of CD133 (green) and LGR5 (red) with counter-staining of DNA (blue) in glioblastoma tumor section. Staining from two independent cases are shown. Scale bar = 20 μm. Astro = cultured normal human astrocytes; CSCs = cancer stem-like cells; NB = normal brain.

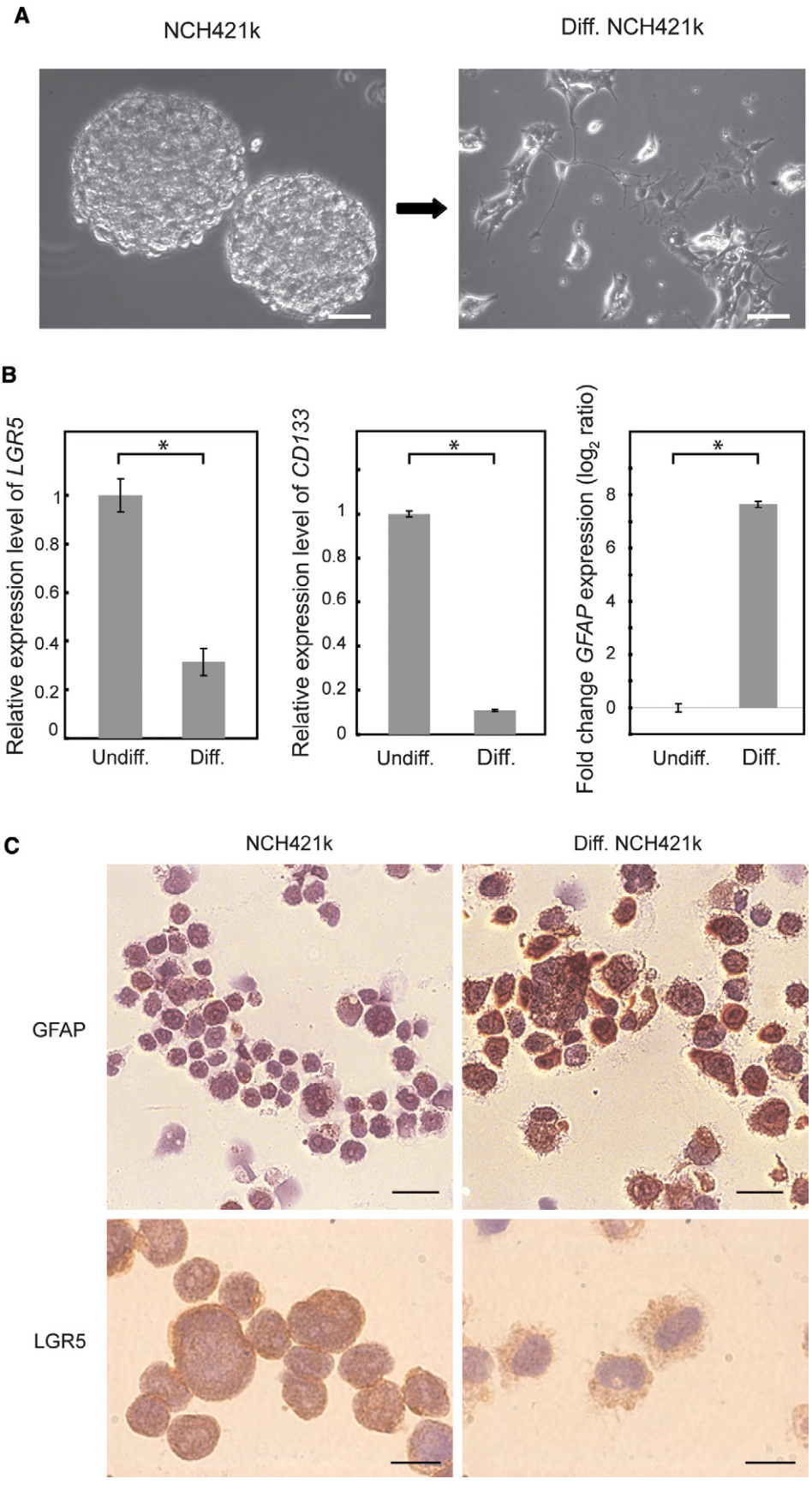

Figure 2. *LGR5 is downregulated upon differentiation.* **A.** Phase contrast images of NCH421k cells before and after induction of differentiation using ATRA. Scale bar = 20 μm. **B.** Analysis of *LGR5*, *CD133* and *GFAP* mRNA expression quantified by quantitative real-time polymerase chain reaction in NCH421k cells and ATRA-differentiated cells. Results were normalized to mRNA levels of two housekeeping genes. Error bars represent standard deviations of three independent biological replicates. **C.** Protein expression of GFAP and LGR5 were visualized by immunohistochemistry in cytospin smears of NCH421k cells and ATRA-differentiated NCH421k cells. Scale bar = 20 μm, GFAP staining; 10 μm LGR5 staining. ATRA = all-trans retinoic acid.

knockdown significantly decreased the number of viable CSCs (Figure 3E) and increased the proportion of trypan blue-positive dead CSCs (Figure 3F). The significant reduction of viability upon silencing of *LGR5* was confirmed by a metabolism-based Cell Titer Glo viability assay (Figure 3D). In order to determine the level of apoptosis, we measured the number of dead cells upon *LGR5* knockdown by flow cytometry. As shown in Figure 3G–I, the size of the subG1 population was significantly increased when compared with the negative control in *LGR5*-silenced NCH421k cells. Similar results were observed in NCH441, an additional CSC line (Supporting Figure S1), indicating the importance of *LGR5* for the survival of brain CSCs *in vitro*. In line with these observations, even 9 days after *LGR5* silencing, sphere formation could not be detected, in contrast to confluent sphere formation in CSC lines transduced with nontarget shRNA (Supporting Information Figure S2).

In ATRA-differentiated cells, no significant rate of apoptosis was observed despite the low *LGR5* expression, suggesting that pro-survival function of *LGR5* might be specific for stem cell cultures maintained in serum-free medium. To exclude that serum-containing components could rescue *LGR5*-silenced cells from apoptosis induction, we cultivated spheroid cells in serum-containing medium. However, these culture conditions failed to attenuate apoptosis induction in *LGR5*-silenced brain CSCs (data not shown), indicating that serum components are not responsible for the survival of *LGR5*-low expressing cells in differentiation promoting conditions.

L1CAM is a downstream target of *LGR5*

Next, we studied the impact of silencing *LGR5* on gene expression of brain CSCs. NCH421k cells were transduced with three different shRNAs targeting *LGR5* and subsequently, the mRNA profiles were compared with those of three negative controls. We performed unsupervised hierarchical clustering of the RNA expression data of un-transduced cells (mock), cells transduced with an empty pLKO.1 vector or with a nontargeting shRNA, as well as the *LGR5* knockdown NCH421k. As depicted by the Euclidean distance, silenced cells were easily distinguishable from three negative controls that cluster together, (Figure 4A).

By SAM, using a false discovery rate and a q-value < 1% as statistical cut-off values, we identified 78 and 27 genes that showed significant down- and upregulation, respectively. By qRT-PCR, we verified the expression of a set of genes that showed downregulation of mRNA expression level upon *LGR5* silencing (Figure 4B). Among them are several genes known to be regulated by environmental factors such as pH and oxygen level (e.g., *CA9, VEGFA, PFKFB4* and *L1CAM*; Tables 1 and 2). However, the high representation of hypoxia-related genes among the differentially regulated genes could be caused by the disruption of the spheric conformation upon the silencing of *LGR5* leading to more normoxic conditions and therefore may result from the specific *in vitro* conditions. To address this question, we used an adherent cell culture system for NSCs maintenance (30). *LGR5*-silenced cells in adherent stem cell culture did not show the significant reduction of *VEGFA, CA9* or *PFKFB4*. In contrast, *L1CAM* was downregulated upon *LGR5* knockdown also in the adherent CSC cultures that are subject to a constant and equal level of oxygen (Figure 4C). Moreover, *LGR5* knockdown induced a significant level of apoptosis in adherent stem cell cultures as well. These results demonstrate that the induction of apoptosis and the downregulation of *L1CAM* caused by *LGR5* knockdown are independent of the sphere formation or the change of the oxygen level.

LGR5 expression correlates with tumor malignancy and is associated with glioblastoma prognosis

Previous reports have established a direct link between patient outcome and levels of expression of putative stem cell markers, such as nestin and CD133 (39–41). In order to study its relevance as potential prognostic marker, LGR5 protein expression was analyzed by immunohistochemistry on a tissue microarray containing tissues derived from 283 different astrocytic glioma samples of WHO grades II–IV (Figure 5A). We identified 34 and 111 cases classified as score 1 and 2, respectively, and defined as low-LGR5 expressing group, as well as a high-LGR5 expressing group encompassing 100 and 9 samples classified as score 3 and 4, respectively.

Interestingly, LRG5 expression correlated with tumor aggressiveness (Pearson's correlation coefficient 0.4, $P < 0.001$) and was higher in glioblastomas (WHO grade IV) as compared with WHO grades II and III astrocytomas, with a high LGR5 expression in 47% of glioblastomas, but only in 13% of WHO grades II and III astrocytomas (Table 3). These results indicate that LGR5 expression increases with malignancy. To further corroborate a function of LGR5 in tumor progression, we investigated the association of LGR5 protein expression with patient survival. Kaplan–Meier analysis showed significant correlation of LGR5 expression with shorter survival ($P < 0.0001$, Figure 5B). Remarkably, when the analysis was restricted to glioblastomas, significant correlation between overall survival and LGR5 protein expression was also observed ($P = 0.0109$, Figure 5C), indicating that LGR5 protein expression is a prognostic marker in glioblastoma. The association with adverse survival was even more pronounced after adjusting for age and gender, two potential clinical confounders ($P = 0.002$).

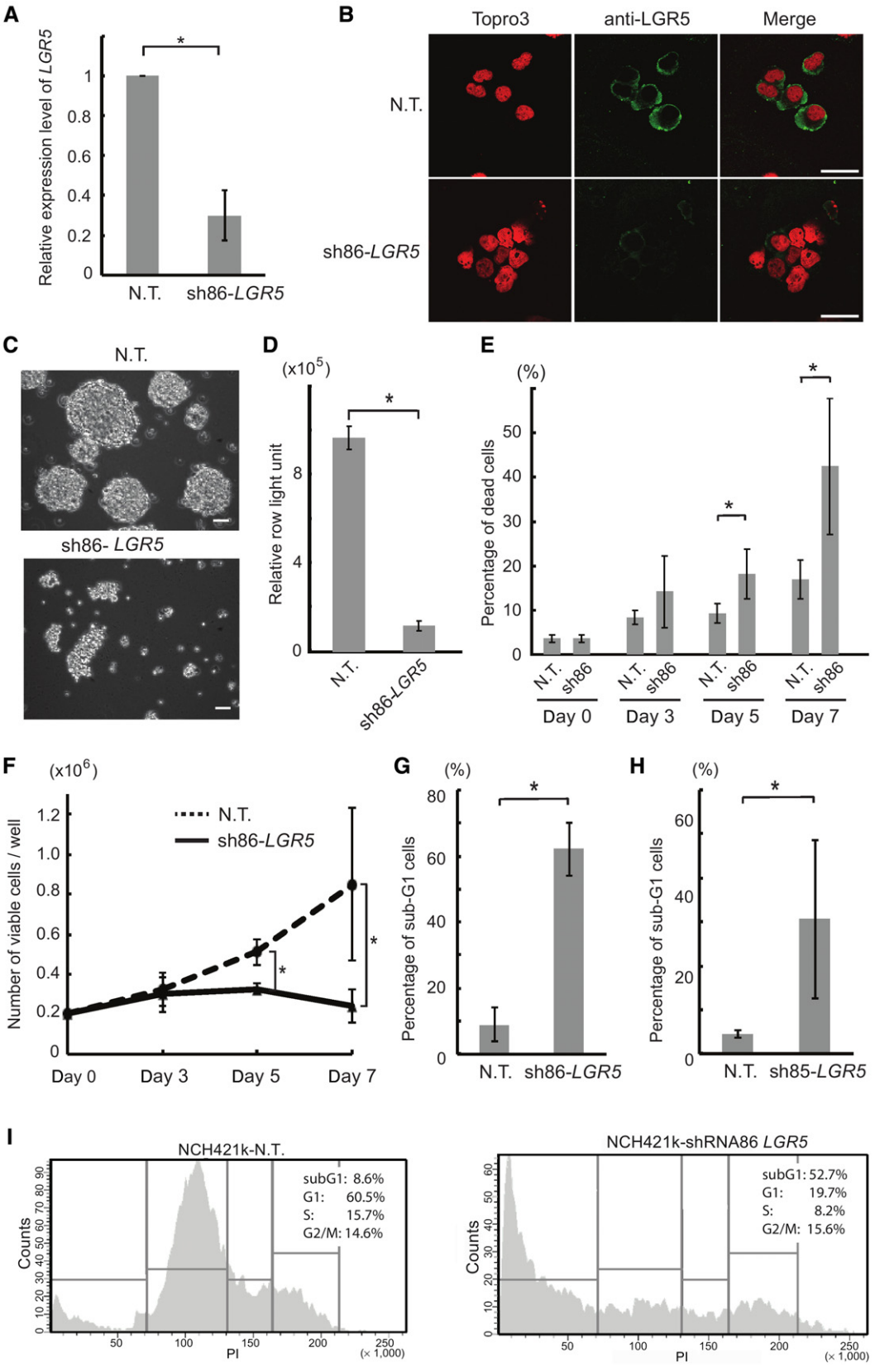

Figure 3. *LGR5 depletion induces apoptosis in brain CSCs.* **A.** Quantitative real-time polymerase chain reaction analysis of *LGR5* mRNA expression in NCH421k cells transduced with lentiviral NT and *LGR5* shRNA (sh-*LGR5*). **B.** Protein expression of LGR5 was visualized by immunofluorescence staining in cytospin smears of NCH421k cells transduced with lentiviral NT and *LGR5* shRNA (sh-*LGR5*). Scale bar = 20 μm. **C.** Phase contrast images of NCH421k and NCH441 cells 7 days after the transduction with NT and *LGR5* lentiviral shRNA. Scale bar; 50 μm. **D.** NCH421k cells were transduced with NT and *LGR5* shRNA and then assessed for viability by CellTiter-Glo assay. Error bars represent the standard deviation of three independent biological replicates. **E–F.** NCH421k cells were transduced with NT and *LGR5* shRNA and then assessed for viability by trypan blue dye exclusion tests on day 0, 3, 5 and 7 days after the transduction. Absolute numbers of trypan blue-negative viable cells were shown in **D**, and percentages of trypan blue-positive dead cells in **E. G–H.** Validation of the apoptosis phenotype upon *LGR5* silencing using two different shRNAs by PI staining and sub-G1 assay in NCH421k. Quantitative analysis of three independent experiments of sub-G1 assay are shown. *P*-value < 0.001, Student's *t*-test. **I.** Representing histograms of sub-G1 assay are shown. Left panel, NT control; Right panel, shRNA targeting *LGR5*. NT = nontarget control.

DISCUSSION

Here, we demonstrate that *LGR5*, a stem cell marker in various tissues, is highly expressed in brain CSCs *in vitro*, when compared with astrocytes and normal brain extracts. Notably, *LGR5* depletion led to strong induction of apoptosis in brain CSCs, indicating a pro-survival role of *LGR5* for this type of stem cells. Moreover, *LGR5* expression was reduced upon cell differentiation by adding

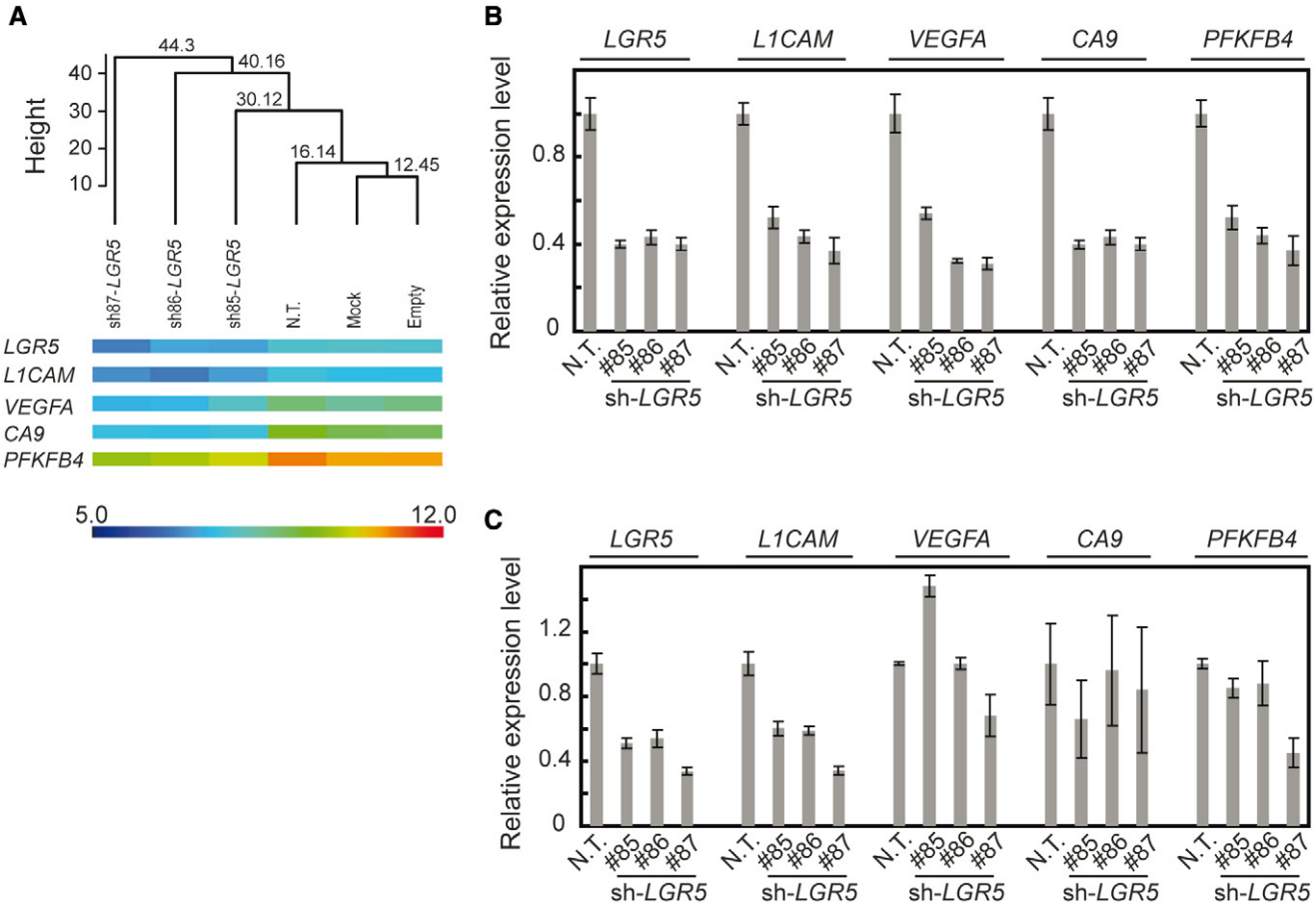

Figure 4. *Expression analysis of LGR5 knockdowns by microarrays.* **A.** Dendogram built upon unsupervised clustering using information from all the probe sets of the microarrays. Three negative controls (Mock, empty vector and nontarget shRNA) and three samples silenced with three different *LGR5* targeting shRNAs were studied by significance analysis of microarrays. The Euclidean distance is represented by the height on the *y*-axis. Heatmaps of the verified genes are depicted. Color scale represents the intensity of the hybridization on Illumina microarrays. **B.** Confirmation of the significant gene expression changes using qRT-PCR in NCH421k cells cultivated in suspension. **C.** Verification of the significant gene expression changes by qRT-PCR in NCH421k cells cultivated in adherent conditions. Error bars represent the standard deviation of three independent biological replicates. qRT-PCR = quantitative real-time polymerase chain reaction.

Table 1. List of genes downregulated upon LGR5 knockdown.

Gene symbol	Gene name	Fold change (Log2)	*q*-value (%)
CA9*	Carbonic anhydrase 9 precursor	–1.54	0
MT3	Metallothionein-3	–1.41	0
NDRG1	N-myc downstreamregulated gene 1 protein	–1.35	0
AHNAK2	AHNAK nucleoprotein 2	–1.26	0
MIA	Melanoma-derived growth regulatory protein precursor	–1.25	0
ZNF395	Zinc finger protein 395	–1.08	0
WSB1	WD repeat and SOCS box-containing protein 1	–1.05	0
PKM2	Pyruvate kinase isozymes M1/M2	–1.04	0
VEGFA*	Vascular endothelial growth factor A precursor	–1.03	0
SLC5A3	Sodium/myo-inositol cotransporter (Na(+)	–1.01	0
RNASE4	Ribonuclease 4 precursor	–0.98	0
MT1A	Metallothionein-1A	–0.92	0
FZD3	Frizzled-3 precursor	–0.92	0
PRRT2	Proline-rich transmembrane protein 2	–0.90	0
C1orf54	Uncharacterized protein C1orf54 precursor.	–0.88	0
ALDOC	Fructose-bisphosphate aldolase C	–0.88	0
PFKFB4*	6-phosphofructo-2-kinase/fructose-2,6-biphosphatase 4	–0.86	0
CCDC136	Coiled-coil domain-containing 136	–0.84	0
MFNG	Beta-1,3-N-acetylglucosaminyltransferase manic fringe	–0.83	0
ATP1A2	Sodium/potassium-transporting ATPase subunit alpha-2 precursor	–0.82	0
GSN	Gelsolin precursor	–0.82	0
PGK1	Phosphoglycerate kinase 1	–0.81	0
SLC6A6	Sodium- and chloride-dependent taurine transporter.	–0.79	0
RAB20	Ras-related protein Rab-20.	–0.79	0
LGR5*	Leucine-rich repeat-containing G-protein coupled receptor 5 precursor	–0.78	0
ATP2B4	Plasma membrane calcium-transporting ATPase 4	–0.78	0
TNNT1	Troponin T	–0.77	0
FCGR2A	Low affinity immunoglobulin gamma Fc region receptor II-a precursor	–0.76	0
PPFIA4	Liprin-alpha-4	–0.76	0
NAT10	N-acetyltransferase 10	–0.74	0
MYO9A	Myosin IXA	–0.72	0
L1CAM*	Neural cell adhesion molecule L1 precursor	–0.67	0
NEDD4L	E3 ubiquitin-protein ligase NEDD4-like protein	–0.65	0
STAT5B	Signal transducer and activator of transcription 5B.	–0.63	0
C12orf57	Putative C10 protein.	–0.63	0
SCD	Acyl-CoA desaturase	–0.61	0
GPR125	Probable G-protein coupled receptor 125 precursor.	–0.61	0
MGLL	Monoglyceride lipase	–0.61	0
FRAS1	Extracellular matrix protein FRAS1 precursor.	–0.60	0
RUNX1	Runt-related transcription factor 1	–0.60	0
CBR3	Carbonyl reductase	–0.60	0
TUB	Tubby protein homolog.	–0.59	0
PHF19	PHD finger protein 19 isoform a	–0.59	0
SLC44A1	Choline transporter-like protein 1	–0.58	0
LPIN1	Lipin-1.	–0.58	0
WDR54	WD repeat protein 54.	–0.57	0
COL9A1	Collagen alpha-1(IX) chain precursor.	–0.57	0
GBE1	1,4-alpha-glucan branching enzyme	–0.55	0
ADCK4	Uncharacterized aarF domain-containing protein kinase 4	–0.55	0
NAV1	Neuron navigator 1	–0.54	0
ADNP2	Zinc finger protein 508.	–0.54	0
MGST3	Microsomal glutathione S-transferase 3	–0.53	0
ARMCX4	Armadillo repeat-containing X-linked protein 4.	–0.53	0
CCDC113	Coiled-coil domain-containing protein 113	–0.51	0
PTCHD1	Patched domain-containing protein 1.	–0.51	0
AHCTF1P	AT-hook-containing transcription factor 1	–0.65	0.6024903
SLC22A17	Brain-type organic cation transporter	–0.63	0.6024903

Table 1. *Continued*

Gene symbol	Gene name	Fold change (Log2)	*q*-value (%)
FLNB	Filamin-B	–0.58	0.6024903
HELZ	Probable helicase with zinc finger domain	–0.50	0.6518747
S100A1	S100 calcium-binding protein A1	–0.87	0.6739722
ENO2	Gamma-enolase	–0.72	0.6739722
S100A10	S100 calcium-binding protein A10	–1.03	0.69155407
MT1X	Metallothionein-1X	–0.90	0.69155407
ADM	ADM precursor	–0.57	0.69155407
HK1	Hexokinase-1	–0.60	0.71647495
ACAD11	Nephrocystin-3.	–0.51	0.71647495
LMO1	LIM domain only protein 1	–0.95	0.7296213
DDIT4	RTP801	–0.59	0.7502709
RAB26	Ras-related protein Rab-26.	–0.92	0.75741637
TMEM45A	Transmembrane protein 45A	–0.68	0.7646992
EFEMP2	EGF-containing fibulin-like extracellular matrix protein 2 precursor	–0.59	0.7646992
MT2A	Metallothionein-2	–0.75	0.8033204
CABIN	Calcineurin-binding protein Cabin 1	–0.55	0.8033204
PFKP	6-phosphofructokinase type C	–0.55	0.8033204
SERTAD2	SERTA domain-containing protein 2	–0.54	0.8033204
EML2	Echinoderm microtubule-associated protein-like 2	–0.58	0.88365245
ODF2	Outer dense fiber of sperm tails 2 isoform 1	–0.55	0.935632
CREB3L2	cAMP responsive element-binding protein 3-like protein 2	–0.53	0.9758125

*Differential expression was verified by quantitative real-time polymerase chain reaction.

Table 2. List of genes upregulated upon LGR5 knockdown.

Gene symbol	Gene name	Fold change (Log2)	*q*-value (%)
TMEFF2	Transmembrane protein with EGF-like and two follistatin-like domains	1.33	0
ARL4A	ADP-ribosylation factor-like protein 4A.	1.09	0
CXCL11	Small inducible cytokine B11 precursor	0.84	0
PKIA	cAMP-dependent protein kinase inhibitor alpha	0.83	0
CTSA	Lysosomal protective protein precursor	0.82	0
ARL4A	ADP-ribosylation factor-like protein 4A.	0.75	0
ZNF789	Zinc finger protein 789 isoform 1	0.68	0
VAMP3	Vesicle-associated membrane protein 3	0.65	0
PAFAH2	Platelet-activating factor acetylhydrolase 2, cytoplasmic	0.57	0
GPX7	Glutathione peroxidase 7 precursor	0.69	0.56403345
ARL6IP1	ADP-ribosylation-like factor 6- interacting protein 1	0.57	0.56403345
LARP7	La-related protein 7	0.56	0.56403345
ST7	Suppression of tumorigenicity 7 isoform a	0.50	0.56403345
COL4A1	Collagen alpha-1(IV) chain precursor	0.94	0.64136064
CDKN1B	Cyclin-dependent kinase inhibitor 1B	0.66	0.6518747
BCAT2	Branched-chain-amino-acid aminotransferase, mitochondrial precursor	0.79	0.7796933
CDH19	Cadherin-19 precursor.	0.61	0.7796933
SH3BGRL	SH3 domain-binding glutamic acid-rich-like protein.	0.74	0.88365245
LASS2	LAG1 longevity assurance homolog 2	0.68	0.88365245
ZHX1	Zinc fingers and homeoboxes protein 1.	0.51	0.88365245
DNAJB9	DnaJ homolog subfamily B member 9	0.59	0.935632
C7orf25	UPF0415 protein C7orf25.	0.51	0.935632
CXCL10	Small inducible cytokine B10 precursor	1.22	0.981836
HN1	Hematological and neurological expressed 1 protein	0.68	0.981836
NOVA1	Neuro-oncological ventral antigen 1	0.58	0.981836
BCL2L12	Bcl-2-like 12 protein	0.54	0.981836
PSL2	Protein SPP-like 2A	0.51	0.981836

ADP = adenosine diphosphate; cAMP = cyclic adenosine monophosphate; EGF = epidermal growth factor; SPP = signal peptide peptidase.

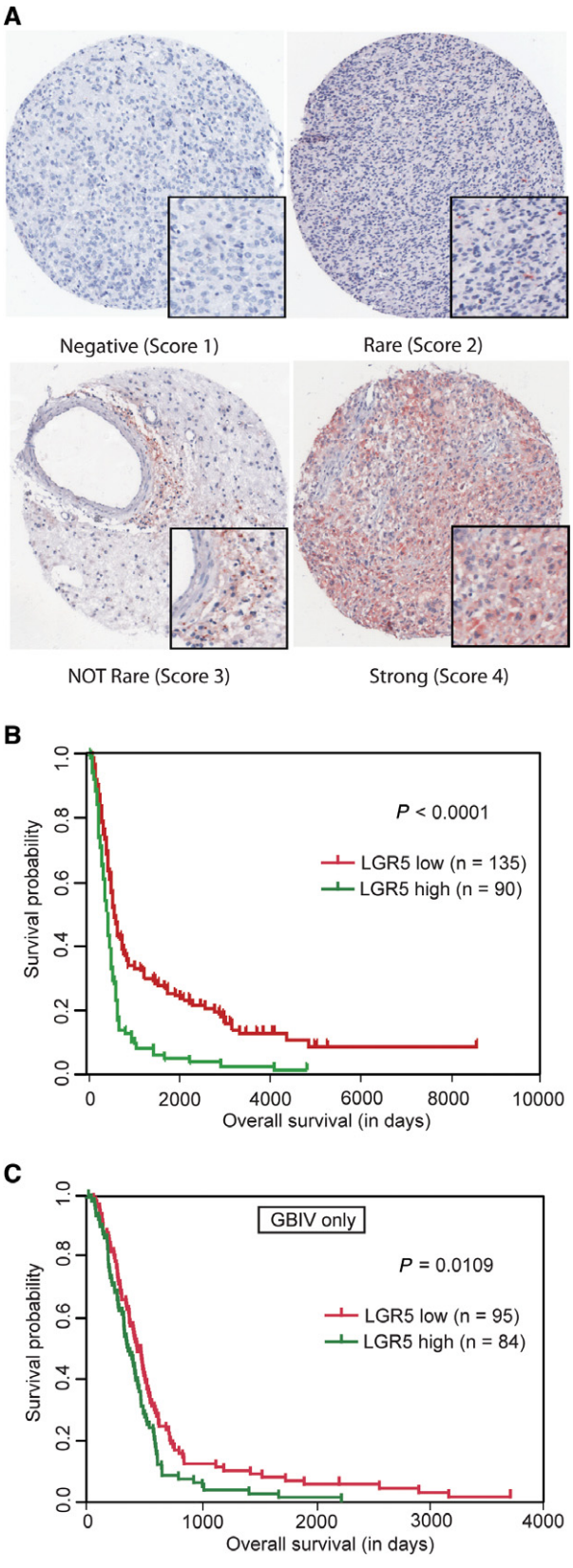

Figure 5. *Expression of LGR5 in gliomas.* **A.** Representative immunohistochemistry staining of LGR5 on tissue microarrays. **B.** Kaplan–Meier analysis showing the significant association of LGR5 expression with overall survival rate in all glioma tumors ($P < 0.0001$). Low- and high-expression groups were separated according to the strength of the staining. Score 1 and 2 were grouped and considered as low expression. Score 3 and 4 represented the sections with a high LGR5 protein expression. **C.** Kaplan–Meier analysis showing the association of LGR5 expression with overall survival in patients with glioblastoma multiforme grade IV ($P = 0.0109$).

serum and ATRA. Together, these data indicate a preferential expression and function of *LGR5* in CSCs.

Several studies have shown the correlation of stem cell marker expression, such as CD133, with the clinical outcome in glioma patients (39–41). In a large panel of glioma sections, we observed that the proportion of cells expressing LGR5 protein increases with tumor grade. Moreover, LGR5 expression in glioblastoma samples was associated with worse clinical outcome, suggesting that content of LGR5-positive cells within each tumor might affect tumor aggressiveness or resistance to therapy. These results indicate that LGR5 could be used as a novel prognostic marker for glioma patients.

By microarray analysis, we demonstrated that knockdown of *LGR5* leads to downregulation of *L1CAM* expression in glioblastoma cells. Interestingly, L1CAM has previously been implicated in CSC maintenance as L1CAM inhibition blocked sphere-forming activity and induced apoptosis in glioblastoma stem cells (3). As *L1CAM* is also one of the downstream target genes of the Wnt pathway (18), we tested whether *LGR5* knockdown attenuates Wnt pathway signaling. However, we did not find any other Wnt pathway target gene, such as *CCND1, cMYC* or *AXIN*, to be downregulated by *LGR5* knockdown. *L1CAM* is also known as an angiogenic gene that is induced by hypoxic treatment (28). Indeed, we observed several hypoxia-related genes downregulated by *LGR5* knockdown in spheroid culture, including *VEGFA, CA9, NDRG1, ALDOC, PGK1* and *PFKFB4*. Hypoxia-related signaling has been reported as an essential pathway for glioblastoma stem cell maintenance *in vitro* and *in vivo* (21, 23, 27, 33). However, we showed that the expression of these hypoxia-responsive genes was decreased because of the reduced capacity of the *LGR5*-knockdown CSCs to form spheres as compared with negative control. By using an adherent stem cell culture system, we demonstrated that *L1CAM*

Table 3. Expression of LGR5 in human gliomas.

Clinical grading	LGR5 expression*	
	Low (%)	High (%)
WHO grade II	87	13
WHO grade III	86	14
WHO grade IV	53	47

*LGR5 expression level of the tumor sections is defined as low when less than 10% of the cells are positive for LGR5. When more than 10% of the tumor sections is positively stained, LGR5 expression is considered as high.
WHO = World Health Organization.

was the only verified gene that showed a significant downregulation upon LGR5 silencing in both *in vitro* systems.

CD133 is known to be a CSC marker of glioblastoma (35, 38), whereas it is reported that the CD133 expression is not always required for glioblastoma stem-like cells (6, 30). Interestingly, we observed that a subpopulation of $CD133^+$ cells in glioblastomas show higher LGR5 expression. This co-localization implies that the combined usage of CD133 and LGR5 as stem cell markers might be useful for the specific isolation of brain CSCs from fresh tumor samples. However, the lack of antibodies, which recognize the extracellular domain of the native protein of LGR5 for living cell sorting impedes fluorescence-activated cell sorting (FACS)-based isolation and analysis of CD133/LGR5-positive subpopulations of CSCs.

Taken together, our data suggest that *LGR5* is indispensable for the propagation and survival of brain CSCs *in vitro*. In addition, LGR5 expression level increases with glioma progression and correlates with adverse outcome, suggesting that the pro-survival and pro-proliferating functions of LGR5 in CSCs would be activated preferentially in less-differentiated gliomas. Further efforts to characterize the physiological role of *LGR5 in vivo* might unveil additional aspects of the biology of brain CSCs.

ACKNOWLEDGMENTS

This work was supported by the German Research Foundation (DFG; LI406/12-1), as well as the German Federal Ministry of Education and Research (BMBF) within the National Genome Research Network NGFNplus (01GS0883, 01GS0884), and a stipend from the Alexander von Humboldt foundation (S.N.). We thank Karsten Richter for useful discussion and support in confocal laser scanning microscopy. We thank Laura Puccio, Frauke Devens, Magdalena Schlotter and Stefanie Hofmann for their technical support.

CONFLICT OF INTEREST

The authors declare that they have no conflict of interest.

REFERENCES

1. Alcantara Llaguno S, Chen J, Kwon CH, Jackson EL, Li Y, Burns DK *et al* (2009) Malignant astrocytomas originate from neural stem/progenitor cells in a somatic tumor suppressor mouse model. *Cancer Cell* **15**:45–56.
2. Bao S, Wu Q, McLendon RE, Hao Y, Shi Q, Hjelmeland AB *et al* (2006) Glioma stem cells promote radioresistance by preferential activation of the DNA damage response. *Nature* **444**:756–760.
3. Bao S, Wu Q, Li Z, Sathornsumetee S, Wang H, McLendon RE *et al* (2008) Targeting cancer stem cells through L1CAM suppresses glioma growth. *Cancer Res* **68**:6043–6048.
4. Barker N, van Es JH, Kuipers J, Kujala P, van den Born M, Cozijnsen M *et al* (2007) Identification of stem cells in small intestine and colon by marker gene LGR5. *Nature* **449**:1003–1007.
5. Barker N, Huch M, Kujala P, van de Wetering M, Snippert HJ, van Es JH *et al* (2010) LGR5(+ve) stem cells drive self-renewal in the stomach and build long-lived gastric units in vitro. *Cell Stem Cell* **6**:25–36.
6. Beier D, Hau P, Proescholdt M, Lohmeier A, Wischhusen J, Oefner PJ *et al* (2007) CD133(+) and CD133(–) glioblastoma-derived cancer stem cells show differential growth characteristics and molecular profiles. *Cancer Res* **67**:4010–4015.
7. Calabrese C, Poppleton H, Kocak M, Hogg TL, Fuller C, Hamner B *et al* (2007) A perivascular niche for brain tumor stem cells. *Cancer Cell* **11**:69–82.
8. Campos B, Wan F, Farhadi M, Ernst A, Zeppernick F, Tagscherer KE *et al* (2010) Differentiation therapy exerts antitumor effects on stem-like glioma cells. *Clin Cancer Res* **16**:2715–2728.
9. Carmon KS, Gong X, Lin Q, Thomas A, Liu Q (2011) R-spondins function as ligands of the orphan receptors LGR4 and LGR5 to regulate Wnt/beta-catenin signaling. *Proc Natl Acad Sci U S A* **108**:11452–11457.
10. Chirasani SR, Sternjak A, Wend P, Momma S, Campos B, Herrmann IM *et al* (2010) Bone morphogenetic protein-7 release from endogenous neural precursor cells suppresses the tumourigenicity of stem-like glioblastoma cells. *Brain* **133**(Pt 7):1961–1972.
11. Clark PA, Treisman DM, Ebben J, Kuo JS (2007) Developmental signaling pathways in brain tumor-derived stem-like cells. *Dev Dyn* **236**:3297–3308.
12. de Lau W, Barker N, Low TY, Koo BK, Li VS, Teunissen H *et al* (2011) LGR5 homologues associate with Wnt receptors and mediate R-spondin signalling. *Nature* **476**:293–297.
13. Dictus C, Tronnier V, Unterberg A, Herold-Mende C (2007) Comparative analysis of *in vitro* conditions for rat adult neural progenitor cells. *J Neurosci Methods* **161**:250–258.
14. Ernst A, Hofmann S, Ahmadi R, Becker N, Korshunov A, Engel F *et al* (2009) Genomic and expression profiling of glioblastoma stem cell-like spheroid cultures identifies novel tumor-relevant genes associated with survival. *Clin Cancer Res* **15**:6541–6550.
15. Freese JL, Pino D, Pleasure SJ (2010) Wnt signaling in development and disease. *Neurobiol Dis* **38**:148–153.
16. Galli R, Binda E, Orfanelli U, Cipelletti B, Gritti A, De Vitis S *et al* (2004) Isolation and characterization of tumorigenic, stem-like neural precursors from human glioblastoma. *Cancer Res* **64**:7011–7021.
17. Garcia JL, Perez-Caro M, Gomez-Moreta JA, Gonzalez F, Ortiz J, Blanco O *et al* (2010) Molecular analysis of ex-vivo CD133+ GBM cells revealed a common invasive and angiogenic profile but different proliferative signatures among high grade gliomas. *BMC Cancer* **10**:454.
18. Gavert N, Conacci-Sorrell M, Gast D, Schneider A, Altevogt P, Brabletz T, Ben-Ze'ev A (2005) L1, a novel target of beta-catenin signaling, transforms cells and is expressed at the invasive front of colon cancers. *J Cell Biol* **168**:633–642.
19. Gentleman RC, Carey VJ, Bates DM, Bolstad B, Dettling M, Dudoit S *et al* (2004) Bioconductor: open software development for computational biology and bioinformatics. *Genome Biol* **5**:R80.
20. Glinka A, Dolde C, Kirsch N, Huang YL, Kazanskaya O, Ingelfinger D *et al* (2011) LGR4 and LGR5 are R-spondin receptors mediating Wnt/beta-catenin and Wnt/PCP signalling. *EMBO Rep* **12**:1055–1061.
21. Goidts V, Bageritz J, Puccio L, Nakata S, Zapatka M, Barbus S *et al* (2012) RNAi screening in glioma stem-like cells identifies PFKFB4 as a key molecule important for cancer cell survival. *Oncogene* **31**:3235–3243.
22. Haegebarth A, Clevers H (2009) Wnt signaling, LGR5, and stem cells in the intestine and skin. *Am J Pathol* **174**:715–721.
23. Heddleston JM, Li Z, McLendon RE, Hjelmeland AB, Rich JN (2009) The hypoxic microenvironment maintains glioblastoma stem cells and promotes reprogramming towards a cancer stem cell phenotype. *Cell Cycle* **8**:3274–3284.
24. Hemmati HD, Nakano I, Lazareff JA, Masterman-Smith M, Geschwind DH, Bronner-Fraser M, Kornblum HI (2003) Cancerous

stem cells can arise from pediatric brain tumors. *Proc Natl Acad Sci U S A* **100**:15178–15183.
25. Ille F, Sommer L (2005) Wnt signaling: multiple functions in neural development. *Cell Mol Life Sci* **62**:1100–1108.
26. Jaks V, Barker N, Kasper M, van Es JH, Snippert HJ, Clevers H, Toftgard R (2008) LGR5 marks cycling, yet long-lived, hair follicle stem cells. *Nat Genet* **40**:1291–1299.
27. Li Z, Bao S, Wu Q, Wang H, Eyler C, Sathornsumetee S *et al* (2009) Hypoxia-inducible factors regulate tumorigenic capacity of glioma stem cells. *Cancer Cell* **15**:501–513.
28. Ong LL, Li W, Oldigs JK, Kaminski A, Gerstmayer B, Piechaczek C *et al* (2010) Hypoxic/normoxic preconditioning increases endothelial differentiation potential of human bone marrow CD133+ cells. *Tissue Eng Part C Methods* **16**:1069–1081.
29. Patapoutian A, Reichardt LF (2000) Roles of Wnt proteins in neural development and maintenance. *Curr Opin Neurobiol* **10**:392–399.
30. Pollard SM, Yoshikawa K, Clarke ID, Danovi D, Stricker S, Russell R *et al* (2009) Glioma stem cell lines expanded in adherent culture have tumor-specific phenotypes and are suitable for chemical and genetic screens. *Cell Stem Cell* **4**:568–580.
31. Saeed AI, Bhagabati NK, Braisted JC, Liang W, Sharov V, Howe EA *et al* (2006) TM4 microarray software suite. *Methods Enzymol* **411**:134–193.
32. Salmaggi A, Boiardi A, Gelati M, Russo A, Calatozzolo C, Ciusani E *et al* (2006) Glioblastoma-derived tumorospheres identify a population of tumor stem-like cells with angiogenic potential and enhanced multidrug resistance phenotype. *Glia* **54**:850–860.
33. Seidel S, Garvalov BK, Wirta V, von Stechow L, Schanzer A, Meletis K *et al* (2010) A hypoxic niche regulates glioblastoma stem cells through hypoxia inducible factor 2 alpha. *Brain* **133** (Pt 4):983–995.
34. Singh SK, Clarke ID, Terasaki M, Bonn VE, Hawkins C, Squire J, Dirks PB (2003) Identification of a cancer stem cell in human brain tumors. *Cancer Res* **63**:5821–5828.
35. Singh SK, Hawkins C, Clarke ID, Squire JA, Bayani J, Hide T *et al* (2004) Identification of human brain tumour initiating cells. *Nature* **432**:396–401.
36. Van der Flier LG, Sabates-Bellver J, Oving I, Haegebarth A, De Palo M, Anti M *et al* (2007) The intestinal Wnt/TCF signature. *Gastroenterology* **132**:628–632.
37. Van Gelder RN, von Zastrow ME, Yool A, Dement WC, Barchas JD, Eberwine JH (1990) Amplified RNA synthesized from limited quantities of heterogeneous cDNA. *Proc Natl Acad Sci U S A* **87**:1663–1667.
38. Vescovi AL, Galli R, Reynolds BA (2006) Brain tumour stem cells. *Nat Rev Cancer* **6**:425–436.
39. Wan F, Herold-Mende C, Campos B, Centner F-C, Dictus C, Becker N *et al* (2011) Expression of stem cell-associated markers and survival in astrocytic gliomas. *Biomarkers* **16**: 136–143.
40. Zeppernick F, Ahmadi R, Campos B, Dictus C, Helmke BM, Becker N *et al* (2008) Stem cell marker CD133 affects clinical outcome in glioma patients. *Clin Cancer Res* **14**:123–129.
41. Zhang M, Song T, Yang L, Chen R, Wu L, Yang Z, Fang J (2008) Nestin and CD133: valuable stem cell-specific markers for determining clinical outcome of glioma patients. *J Exp Clin Cancer Res* **27**:85.

SUPPORTING INFORMATION

Additional Supporting Information may be found in the online version of this article:

Figure S1. *LGR5 depletion induces apoptosis in another brain CSC line, NCH441 cells.* **A.** qRT-PCR analysis of *LGR5* mRNA expression in NCH441 cells transduced with lentiviral nontarget control shRNA (N.T.) and *LGR5* shRNA (sh-*LGR5*). **B.** Left panel; Phase contrast images of NCH441 cells 7 days after the transduction with nontarget (N.T.) and *LGR5* lentiviral shRNA. Scale bar; 50 μm. Right panel; Macroscopic images in 6 well plates of NCH441k cells 9 days after the transduction with nontarget and *LGR5* lentiviral shRNA. **C.** Validation of the apoptosis phenotype upon *LGR5* silencing by PI staining and Sub-G1 assay in NCH441k.
Figure S2. *LGR5-silenced brain CSCs could not form spheres due to massive cell death.* Macroscopic images of NCH421k cells 9 days after the transduction with nontarget (left panel) and LGR5 lentiviral shRNA (right panel) in a 6 well plate.
Table S1. List of primers used for qRT-PCR.
Table S2. Patient characteristics of astrocytic glioma samples on the tissue microarrays (TMAs).